Volume 18, Number 2, 2025. pp. 241-248

Jordan Journal of Physics

ARTICLE

Coupling Concept for Cross-Bar H-Type Cavities

Ali M. Almomani[a] and **Ulrich Ratzinger**[b]

[a] *Physics Department, Faculty of Science, Yarmouk University, 211-63 Irbid, Jordan.*
[b] *Institute for Applied Physics, J. W. Goethe University, Max-von-Laue Str. 1, 60438 Frankfurt am Main, Germany.*

Doi: **https://doi.org/10.47011/18.2.12**
Received on: 16/01/2024; *Accepted on: 06/03/2024*

Abstract: Crossbar H-type cavities (CH-cavities) have been investigated in the last two decades in different laboratories. They have promising features when compared with conventional drift tube linac (DTL) structures in terms of field gradient, shunt impedance, and costs. The KONUS beam dynamics concept allows for short drift tube sections without focusing lenses, resulting in a limited number of gaps per CH-cavity. With the available 3 MW klystron, the short cavity structure does not use the full amplifier power. Therefore, the RF- coupling of two single cavities seems to be an applicable solution to have more gaps per structure without harming the beam dynamics. This concept is realized by coupling three resonators and operating them as a single structure in the zero mode. In this paper, two identical CH tanks—each with 13 gaps—are coupled using a coupling cell containing a quadrupole triplet. The results are compared with theory. This type of cavity is called a coupled CH-cavity (CCH). The design frequency and field distribution result from an optimization of the three coupled resonators and are described in this paper. The fine-tuning is done by fixed and movable tuners along the structure.

Keywords: Drift tube linac, Coupled CH cavity, KONUS beam dynamics.

1. Introduction

H-type structures [1] are an alternative to the conventional drift tube linac (DTL) at energies up to around 100 MeV per nucleon (A MeV). “H-mode” and “TE-mode” are equivalent designations for modes with an H-field component along the direction of wave propagation. In these structures, a combination of slim, lens-free drift tubes with the Kombinierte Null Grad Struktur (Combined Zero-Degree Structure, KONUS) beam dynamics [2] allows for reaching a high effective field gradient and a high shunt impedance at modest structural costs [3, 4, 5].

In contrast to the Alvarez DTL (E010-mode), the electric field lines in H-type cavities without a drift tube structure are oriented transversally to the beam axis [1]. Fig. 1 shows the electric and magnetic fields of a pillbox cavity excited in H_{211} mode, based on CST-MW calculations [6]. All simulations in this paper were performed using this commercial software.

Since the axial electric field required for particle acceleration is zero in empty H-type cavities, one has to introduce a sequence of drift tubes along the cavity axis. These drift tubes are connected to the cavity tank wall by stems. This array generates the longitudinal electric field for beam acceleration. H-type structures have excellent properties in terms of RF efficiency, beam quality, operation reliability, and cost efficiency, making them attractive for low and medium β-acceleration. Two kinds of structures are realized and operated as H-modes: IH- and CH-DTLs (Fig. 2).

Corresponding Author: Ali M. Almomani **Email**: ali.almomani@yu.edu.jo

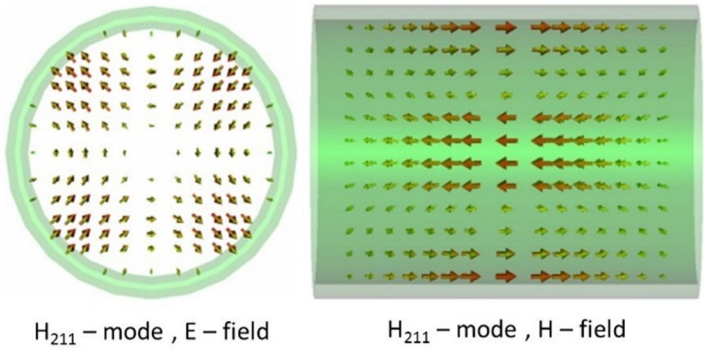

FIG. 1. Electric and magnetic field distributions for the H_{211}-mode in a pillbox cavity.

FIG. 2. Views into IH-DTL (left) and CH-DTL (right) cavities.

In the low beta range, the interdigital (IH) DTL can be used to accelerate particles up to a normalized velocity of $\beta = v/c \approx 0.25$ [1]. The operational frequency for such cavities was below 300 MHz so far. Beyond this point, the dimensions of the IH-DTL are too small, and the mechanical design becomes very difficult to realize. Thus, at higher β, one can use the crossbar H-type (CH) DTL in the H_{211} or H_{210} mode. The cavity dimensions are convenient for frequencies between 150 and 600 MHz [7, 8]. CH-cavities have been investigated by IAP-Frankfurt, GSI-Darmstadt, and LANL in Los Alamos [9]. Moreover, the new FAIR proton injector, currently under construction, is based on CH structures [10].

The available 3 MW klystrons encourage increasing the number of gaps per CH-cavity in order to take advantage of using this power. But, due to the KONUS beam dynamics, which couples short, lens-free accelerating sections by quadrupole triplets, the gap numbers in each section are limited. Consequently, RF-coupling of two CH sections by a coupling cell that contains a quadrupole lens presents an attractive solution. It allows to have similar power requests in each cavity, which fits well with the power level of an industrial amplifier (in our case, a 3 MW klystron). This concept is used in the first three cavities of the FAIR proton linac [3, 10, 11]. In this paper, the applied coupling concept based on theory and simulations is discussed.

2. Coupling Structures Concept

To understand the physical concept of coupled CH sections, coupled by a lens-containing drift tube, consider a system of three magnetically coupled oscillators, as shown in Fig. 3 [12]. Each oscillator has the same frequency ω_0, which is defined as

$$\omega_0 = 1/\sqrt{L_0 C_0} \quad (1)$$

where L_0 is the resonator inductance and C_0 is the resonator capacitance.

This is a very simplified model of our situation.

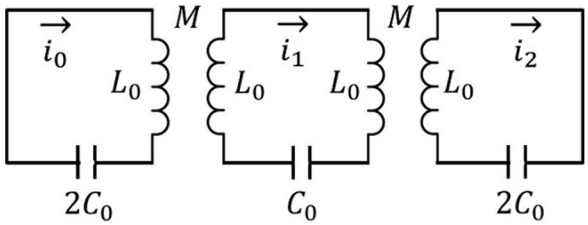

FIG. 3. A system of three magnetically coupled resonators [12], where M is the mutual inductance, L_0 is the resonator inductance, and i_0, i_1, and i_2 are the currents in each resonator.

The first and third oscillators represent the two CH accelerating sections, while the central oscillator represents the coupling section, which contains the magnetic quadrupole triplet.

The central oscillator is coupled with the other two oscillators by a mutual inductance M with a coupling strength that is defined as the ratio between the mutual inductance and the resonator inductance L_0. This is the coupling constant:

$$k = M/L_0 \tag{2}$$

Applying Kirchhoff's laws to this system leads to a system of coupled equations [12]. By solving these equations, one can find three eigenmodes:

- Zero mode, where all oscillators oscillate in phase at a frequency of

$$\Omega_0 = \frac{\omega_0}{\sqrt{1+k}} \tag{3}$$

- $\pi/2$ −mode, where the two accelerating sections at each end oscillate in opposite phase compared to the zero mode. The frequency is

$$\Omega_{\pi/2} = \omega_0 \tag{4}$$

The coupling cell in between shows zero amplitude in this case.

- The π −mode, where all sections are shifted against each other by π. The mode frequency is

$$\Omega_\pi = \frac{\omega_0}{\sqrt{1-k}} \tag{5}$$

The frequency difference between π −mode and 0 −mode is defined as the bandwidth and is given in a good approximation at small k by

$$\delta\omega = \Omega_\pi - \Omega_0 \approx k\omega_0 \tag{6}$$

In the following sections, the coupled CH-DTL is simulated with the commercial package CST-MW [6], and the results are compared to this model. CST-MW is a versatile 3D simulation tool for fast and accurate 3D electromagnetic simulation of high-frequency problems.

3. Concept of Coupled CH (CCH) – Cavity

To show the coupling concept without the disturbance by a real drift tube structure with its beta-profile, we simplified the geometry with respect to that point. The simulated CCH cavity has 26 gaps in total, and the energy profile is constant. For this investigation, the cavity structure consists of two identical accelerating sections, each has 13 accelerating gaps, and the coupling cell in between is 2βλ long in this example. The layout of the cavity is shown in Fig. 4, and Table 1 shows the main cavity parameters.

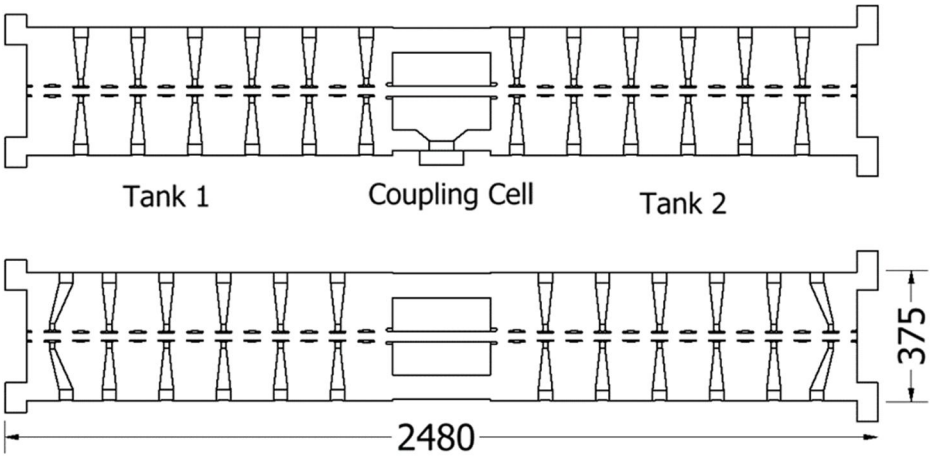

FIG. 4. Layout of the constant beta CCH cavity showing the main dimensions.

TABLE 1. Main parameters of the coupled CH cavity.

Number of Gaps	26
Design Frequency (MHz)	325.224
Eff. Accel. Length (mm)	2480
Shunt Impedance Z_0 (MΩ/m)	84.4
Q_0 – value	14400
Drift tube Aperture (mm)	20
Lens Aperture (mm)	20
$\Delta f_{\pi/2} = f_{\pi/2} - f_0$ (kHz)	700
$\Delta f_{\pi} = f_{\pi} - f_0$ (kHz)	4700

RF simulations show that the two CH tanks are coupled efficiently after optimizing the cavity and coupling cell dimensions. The coupling in such a CCH cavity is achieved after tuning each of the three cavity parts separately to the operating frequency.

When the three coupled oscillators model from section 2 is applied to this cavity, one can derive the coupling factor from the resonance frequencies of the three lowest modes as described in Eq. (5). This results in k = 0.011. On the other hand, one can compare the frequency shift between π – mode and 0 – mode, and π/2 – and 0 – mode, which is asymmetric as can be seen in Table 1. This is a hint that the three coupled oscillators model does not apply very well. The explanation is given below through the analysis of the gap voltage distribution for the three lowest cavity modes.

Another tuning subject was the field tuning at the end cells of the cavity, to reach a zero-like mode $H_{21(0)}$.

To solve this issue, the end shapes in the cavity were modified as shown in Fig. 4. By increasing the cavity diameter locally, the inductance is increased to get the end cells in resonance. As a result, the electric fields in the end gaps increased by a factor of two. By that method, the matched cavity ends become short, allowing for an improved mechanical integration of the inter-tank quadrupole triplets. Short drift lengths between cavities improve the longitudinal beam dynamics, as the bunch length can be kept short. Fig. 5 shows the on-axis electric field for the final cavity design in the operating mode (quasi-zero mode). It was calculated by CST-MW. The same curve can be measured by bead-pull measurements along the beam axis of a cavity. The peaks show the field distribution $|E_z(z)|$ along all gaps. The effective shunt impedance increases as well with the new end shapes by 15%, as the total cavity length is reduced.

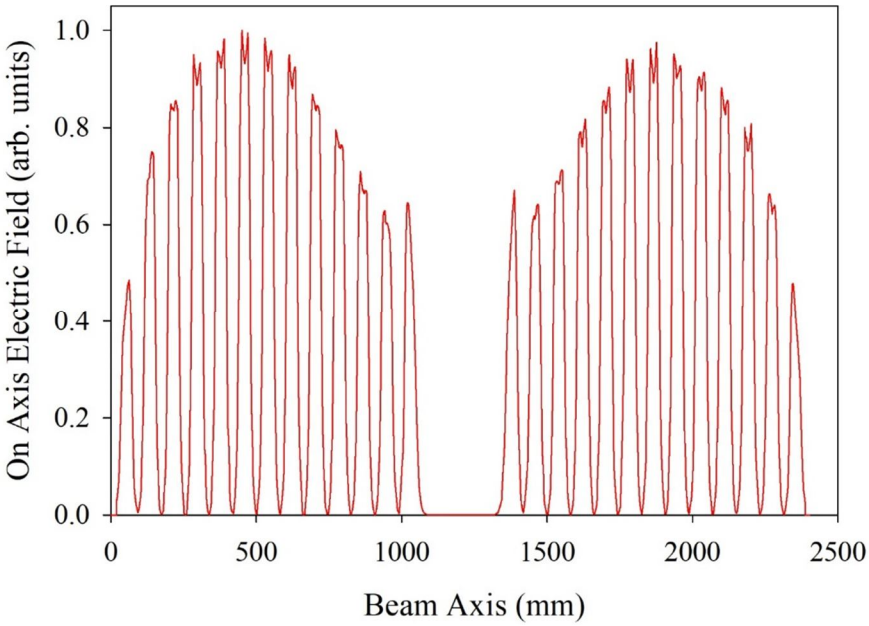

FIG. 5. The absolute on-axis electric field $|E_z(z)|$ distribution along the CCH cavity in quasi-zero-mode.

The effective gap voltage distribution is calculated from the longitudinal electric field distribution by applying the transit time factors for each gap. The results are shown in Fig. 6. The transit time factors can be either obtained from the LORASR beam dynamics code [13] or calculated from the CST field distribution. This controlled process is repeated until the gap voltage deviation between the two distributions falls below approximately 2%. Final optimization of the cavity's field distribution and simulated gap voltages in the beam dynamics code is achieved by inductive tuners (see next section). The 3D electric field distribution of the CCH cavity for the zero mode is shown in Fig. 7.

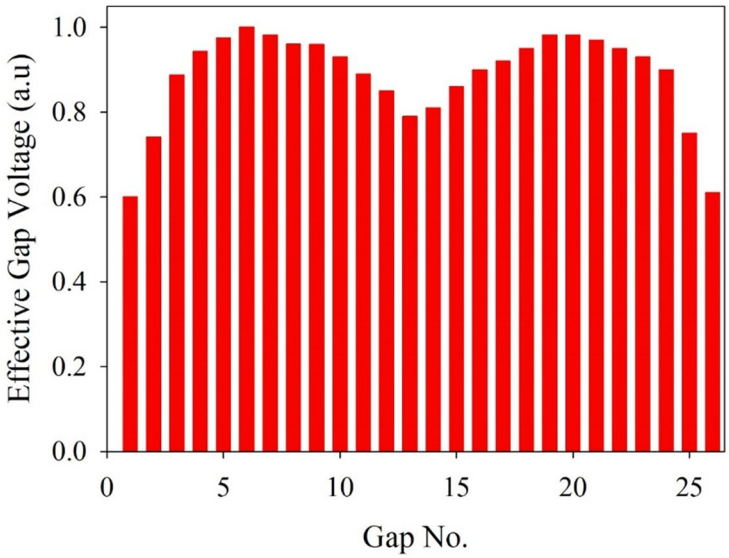

FIG. 6. Effective gap voltage distribution from field simulations by CST-MW.

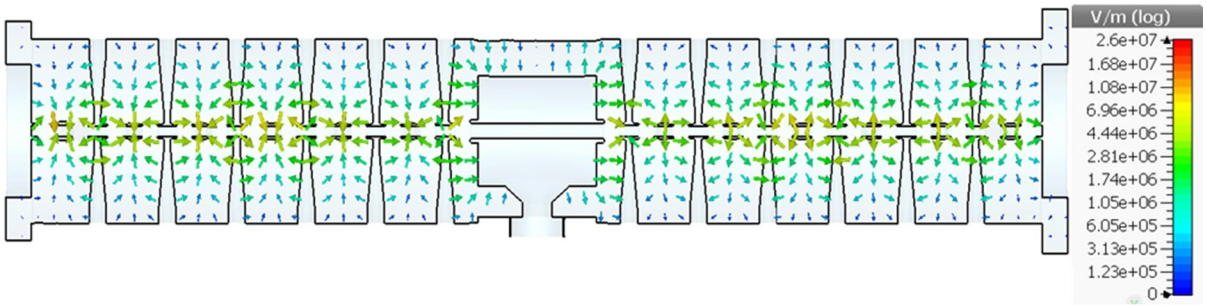

FIG. 7. The 3D electric field distribution along the yz symmetry-plane for the CCH cavity.

As mentioned before, the two CH-drift tube sections are coupled by the coupling cell containing a quadrupole triplet which oscillates in Alvarez mode (E_{010} – mode), as shown in Figs. 8 and 9.

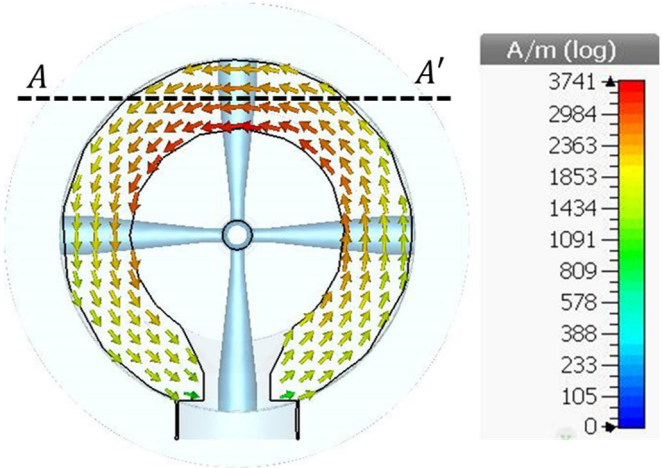

FIG. 8. The magnetic field distribution in the middle plane of the coupling cell.

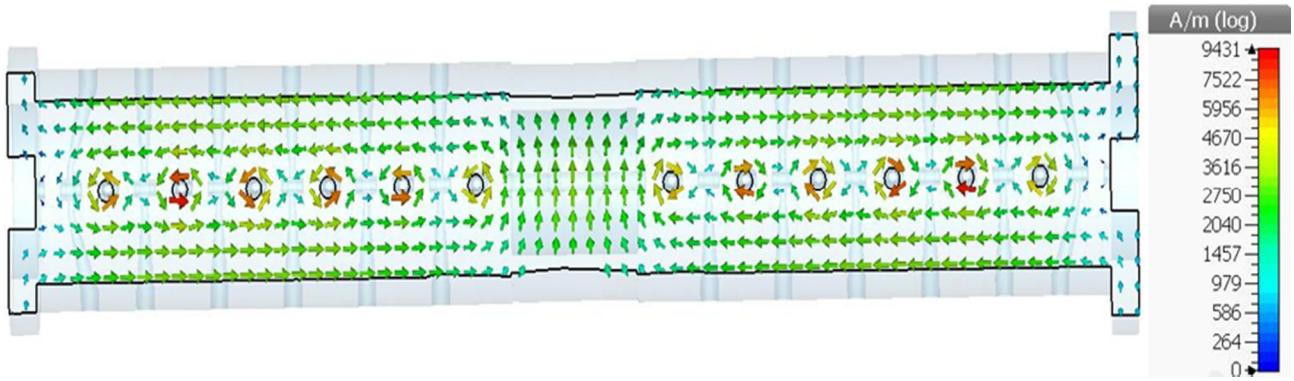

FIG. 9. Magnetic field distribution in shifted xz −plane (AA' in Figure 8) for the CCH cavity.

The magnetic field lines within each quadrant of the drift tube sections are parallel and antiparallel to the beam axis (Fig. 9). Around the coupling lens, however, the angular field direction is dominating. Additionally, the local field lines around the stems are clearly visible in Fig. 9.

The on-axis electric field distributions for the $\pi/2$ – and π – modes are shown in Figs. 10 and 11. Fig. 10 shows that each of the three coupled resonators oscillates with phase relations in the central parts fitting to this simplified model at a first glance. However, the phase relations along the cells of each drift tube section are changed significantly. Although the beta lambda half cells of an H-type structure are coupled very strongly to each other, with coupling constants k typically about 0.3 [14], the phase modulation within each drift tube section plays an important role for the CCH cavity. This should explain why the three coupled oscillators model does not apply too well. Alternative descriptions of the CCH cavity are under development.

The design operating frequency of the investigated coupled CH cavity in this study is 325.224 MHz. For field and gap voltage final tuning, one may apply inductive tuning by cylindrically shaped plungers mainly, as this technique does not influence locally the high electric field regions near the aperture. Moreover, the simple cylindrical tuner body and its short length make cooling easy, and there is no risk of harming the mechanical tuner's vibrations. Also, multipacting is not critical.

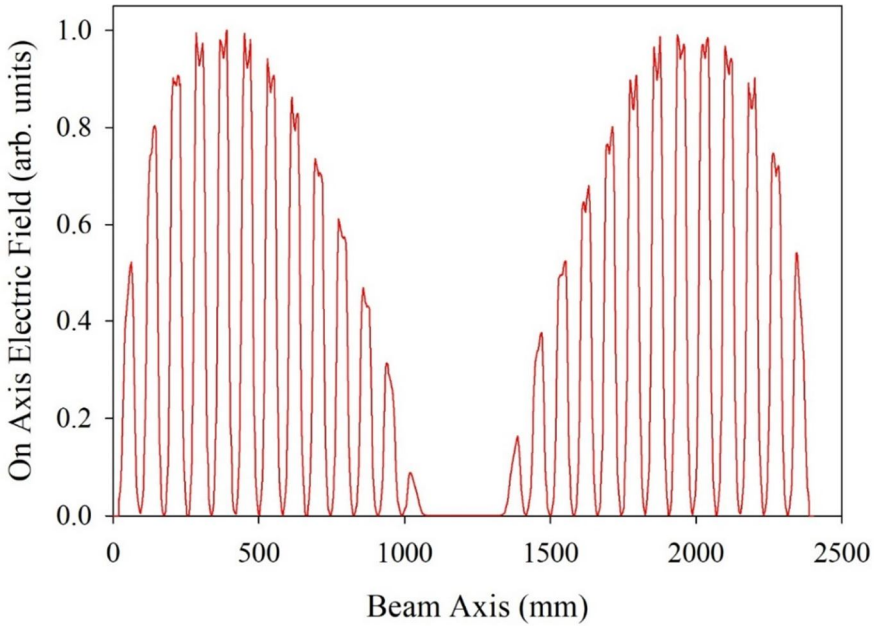

FIG. 10. The absolute on-axis electric field $|E_z(z)|$ distribution along the CCH cavity in $\pi/2$ – mode.

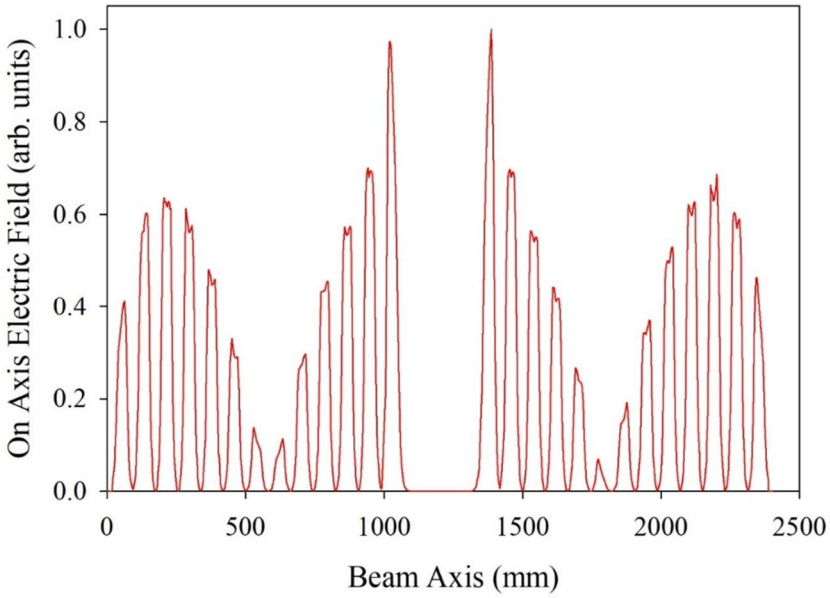

FIG. 11. The absolute on-axis electric field $|E_z(z)|$ distribution along the CCH cavity in π – mode.

In a first rough consideration, it is assumed that the relative frequency shift $\Delta\omega_0/\omega_0$ is proportional to the relative volume change of the cavity $\Delta V_{tuner}/V_{cavity}$, which is valid in the case of a constant absolute magnetic field value in the whole cavity volume:

$$\frac{\Delta\omega_0}{\omega_0} = \frac{\Delta U_m}{U_c} \cong \frac{\Delta V_{tuner}}{V_{cavity}} \tag{7}$$

where ΔU_m is the magnetic field energy in the displaced plunger volume, while U_c denotes the stored cavity field energy. For the cavity volume estimation, the cylindrical cavity volume between the two outer gap centers was taken.

A comparison with the simulations for the coupled CH cavity shows that, for the linear part of the curves in Fig. 12, the following approximation is valid:

$$\frac{\Delta\omega_0}{\omega_0}(simulations) \cong 0.7\frac{\Delta V_{tuner}}{V_{cavity}}\ ; \tag{8}$$

Figure 12 shows the frequency shift against the tuner depth in the case of the CCH cavity. In this simulation, a total of five cylindrical tuners, with a diameter of 60 mm, were moved in parallel. Two of them acted on each drift tube section, while the fifth one acted against the internal lens. The slope up to a tuner length of 40 mm agrees well with Eq. (8). At increased tuner length, the tuner head enters a region with increasing electric field density, resulting in a reduced frequency increase and finally in a decrease when the electric field density is dominating. It is intended to use the most efficient tuning range, up to around 80 mm.

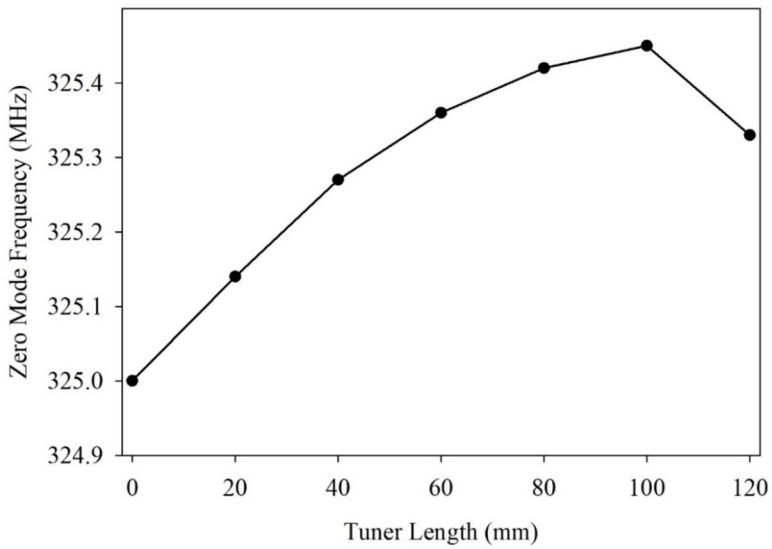

FIG. 12. Simulated frequency shifts by parallel action of five tuners along the coupled CH cavity.

While the field and frequency are fine-tuned by fixed tuners, frequency control during operation is handled by a single mobile tuner which acts within a small tuning range, as the CH cavity temperature is controlled by intensive water-cooling.

4. Conclusion

The coupling of two CH cavities is an important issue for the low-energy part of a CH-DTL. Developments in H-type cavities (IH-DTL and CH-DTL) over the past decades have led to a robust and efficient class of cavities, which can serve as an attractive alternative to the Alvarez DTL in many cases.

To have short drifts between accelerating sections for placing quadrupole lenses and to allow a match of RF power requirements and attractive RF amplifier solutions, the coupling of short CH structures is helpful in the low-energy part of DTL. The coupling method was tested by a simplified three coupled resonators model. The details of the RF coupling of two CH tanks by a coupling cell $2\beta\lambda$ in length containing a triplet lens were described by simulation results.

It has been shown that the fine tuning of a CCH cavity can be accomplished by fixed cylindrical volume tuners.

The concept described in this paper enables the realization of a CH-DTL with KONUS beam dynamics. At the same time, the largest available RF amplifiers of the 3 MW class can be efficiently coupled one by one to the cavities by using CCH cavities at lower beam energies.

References

[1] Ratzinger, U., "H-type Linac Structures", In: Proc. CAS CERN Accelerator School, Radio Frequency Engineering, Seeheim, Germany, 8-16 May 2000, ISBN 92-9083-249-5, p. 351 – 379.

[2] Ratzinger, U., Hähnel, H., Tiede, R., Kaiser, J., and Almomani, A., Phys. Rev. Accel. Beams, 22 (2019) 114801.

[3] Ratzinger, U., A Low Beta RF Linac-Structure of the IH-type with Improved Radial Acceptance, in Proc. 1988 Linear Accelerator Conference (LINAC'88) Newport News, VA (JACoW, Geneva, 2003), p. 185.

[4] Clemente, G. et al., Phys. Rev. Accel. Beams, 14, (2011) 110101.

[5] Broere, J., Kugler, H., Vertenar, M., Rarzinger, U., and Krietenstein, B., High Power Conditioning of the 202 MHz IH Tank 2 at the CERN LINAC3, Proc. LINAC98, Chicago, USA, p. 771 (1998).

[6] CST MICROWAVE. http://www.cst.com/.

[7] Ratzinger, U., The New High Current Ion Accelerator at GSI and Perspectives for Linac Design Based on H-mode Cavities, in Proc. European Particle Accelerator Conf., Vienna, 2000 (EPS, Geneva, 2000), pp. 98–102.

[8] Almomani, A. and Ratzinger, U., Status of a 325 MHz High Gradient CH - Cavity, in Proceedings of 28th Linear Accelerator Conf. (LINAC'16), East Lansing, MI, USA, THPLR059, pp. 982-984 (2016).

[9] Carneiro, J.-P., Mustapha, B., and Ostroumov, P.N., Nucl. Instrum. Methods Phys. Res., Sect. A, 606, (2009) 271.

[10] Almomani, A., Busch, M., Dziuba, F.D., Kleffner, C.M., Ratzinger, U., and Tiede, R., Journal of Physics: Conference Series, 874 (2017) 012046.

[11] Brodhage, R., Vinzenz, W., Clemente, G., and Ratzinger, U., First Coupled CH Power Cavity for the FAIR Proton Injector, in Proceedings of the 5th International Particle Accelerator Conference IPAC14, Dresden, Germany, pp. 3232–3234 (2014).

[12] Wangler, T., "RF Linear Accelerators", 2nd Ed., (Wiley-VCH Verlag GmbH & Co. KGaA, Weinheim, 2008).

[13] Tiede, R., Clemente, G., Podlech, H., Ratzinger, U., Sauer, A., and Minaev, S., LORASR Code Development, in Proceedings of the European Particle Accelerator Conference EPAC06, Edinburgh, Scotland, WEPCH118, pp. 2194-2196 (2006).

[14] Lapostolle, P.M. and Septier, A.L., "Linear Accelerators", North Holland Publishing Company, 1970; ISBN, 0720401569, 9780720401561.